Geminate Proton Recombination at the Surface of SDS and CTAC Micelles Probed with a Micelle-Anchored Anthocyanin

ARTICLE *in* LANGMUIR · FEBRUARY 2006

Impact Factor: 4.46 · DOI: 10.1021/la0522911 · Source: PubMed

Geminate Proton Recombination at the Surface of SDS and CTAC Micelles Probed with a Micelle-Anchored Anthocyanin

Rita Rodrigues,[†] Carolina Vautier-Giongo,[‡] Palmira F. Silva,[†] Ana C. Fernandes,[§] Rui Cruz,[§] António L. Maçanita,[†] and Frank H. Quina*[,‡]

Centro de Química Estrutural, Departamento Engenharia Química, IST/UTL, Lisboa, Portugal, Instituto de Química, Universidade de São Paulo, CP 26077, São Paulo 05513-970, Brazil, and Instituto de Tecnologia Química e Biológica, UNL, Oeiras, Portugal

Received August 22, 2005. In Final Form: November 11, 2005

The functionalized flavylium salt 6-hexyl-7-hydroxy-4-methyflavylium chloride (HHMF) was employed to probe some of the fundamental features of proton transfer reactions at the surface of anionic sodium dodecyl sulfate (SDS) and cationic hexadecyltrimethylammonium chloride (CTAC) micelles. In contrast to most ordinary flavylium salts, HHMF is insoluble in water, but readily incorporates into SDS and CTAC micelles. In the ground state, the rate constant for deprotonation of the acid form (AH^+) of HHMF decreases 100-fold upon going from CTAC ($k_d = 3.0 \times 10^6\ s^{-1}$) to SDS ($k_d = 1.4 \times 10^4\ s^{-1}$), consistent with the presence of an activation barrier for proton transfer in the ground state and reflecting, respectively, stabilization or destabilization of the AH^+ cation by the micelle. Reprotonation of A is diffusion-controlled in both micelles ($k_p(SDS) = (2.1 \times 10^{11})[H^+]_{aq}\ s^{-1}$ and $k_p(CTAC) = (3.7 \times 10^8)[H^+]_{aq}\ s^{-1}$), the difference reflecting the rate of proton entry into the micelles. In the excited singlet state, the rate constants for deprotonation of the $AH^{+}*$ form of HHMF are similar in the two micelles ($2.4 \times 10^{10}\ s^{-1}$), consistent with activationless proton transfer. Reprotonation of the excited A* is dominated by fast geminate recombination of the photogenerated (A^*-H^+) pair at the micelle surface ($k_{rec}(SDS) = 6.1 \times 10^9\ s^{-1}$ and $k_{rec}(CTAC) = 3.4 \times 10^{10}\ s^{-1}$) and the net efficiencies of geminate recombination are quite similar in SDS (0.89) and CTAC (0.86).

Introduction

Proton and electron transfer in heterogeneous media play a central role in a number of chemical and biological processes.[1,2] In such media, the parameters controlling the efficiency of these two processes (dielectric constant, viscosity, redox potentials, etc.) may differ substantially from those in homogeneous solvents.[3] An understanding of the role of these parameters from a fundamental molecular perspective is crucial for modeling these reactions in nonhomogeneous media such as those present in biological systems.

At the interface of self-organized assemblies, both the viscosity and static polarity of the medium differ considerably from those in bulk water[4−6] and confinement[7] imposes considerable restraints on the movement of reactants. The average local proton concentration in the interface is lower in cationic micelles and higher in anionic micelles than that in the intermicellar bulk aqueous phase,[8] and the equilibrium and rate constants for ground- and excited-state proton transfer reflect both the effective proton concentration and the relative degree of stabilization or destabilization of the species involved.[9−11] As a consequence, one might expect the kinetics and energetics of proton transfer processes taking place at the interface of the micelles to be drastically affected, particularly at the charged interface of ionic micelles.[8]

Synthetic hydroxyflavylium cations are particularly appropriate for probing the dynamics of both proton and electron transfer.[9−16] The proton transfer rate constants of these compounds can be readily evaluated in both the ground (microsecond time range)[9,10,14] and excited (picosecond time range),[11,12,14] states and their fluorescence is efficiently quenched by relatively poor electron donors, reflecting the extraordinarily high electron affinity of the flavylium cation.[15,16] Consequently, flavylium salts should be sensitive probes for the investigation of proton availability and mobility in microenvironments over a wide time range (picoseconds to milliseconds) and of medium effects on electron transfer in these environments. Indeed, the rate constant for

* Address correspondence to this author. Telephone: ++55−11-3091-2162. Fax: ++55-11-3815-5570. E-mail: quina@usp.br or frhquina@iq.usp.br.

[†] IST/UTL.

[‡] Universidade de São Paulo.

[§] UNL.

(1) (a) Fendler, J. H.; Fendler, E. J. *Catalysis in micellar and macromolecular systems*; Academic Press: New York, 1975. (b) Fendler, J. H. *Membrane mimetic chemistry: characterizations and applications of micelles, microemulsions, monolayers, bilayers, vesicles, host−guest systems, and polyions*; Wiley: New York, 1982.

(2) (a) Kalyanasundaram, K. *Photochemistry in microheterogeneous systems*; Academic Press: Orlando, 1987. (b) Grätzel, M.; Kalyanasundaram, K. *Kinetics and catalysis in microheterogeneous systems*; Marcel Dekker: New York, 1991. (c) Gehlen, M. H.; De Schryver, F. C. *Chem. Rev.* **1993**, *93*, 199−221.

(3) Pramauro, E.; Pelizzetti, E. *Surfactants in Analytical Chemistry*—Applications of Organized Amphiphilic Media; Elsevier: Amsterdam, 1996.

(4) (a) El Seoud, O. A. *J. Mol. Liq.* **1997**, *72*, 85−103. (b) Possidonio, S.; Siviero, F.; El Seoud, O. A. *J. Phys. Org. Chem.* **1999**, *12*, 325−332. (c) Novaki, L. P.; El Seoud, O. A. *Langmuir* **2000**, *16*, 35−41.

(5) Bales, B. L.; Zana, R. *J. Phys. Chem. B* **2002**, *106*, 1926−1939.

(6) Grieser, F.; Drummond, C. S. *J. Phys. Chem.* **1988**, *92*, 5580−5593.

(7) Weiss, R. G.; Ramamurthy, V.; Hammond, G. S. *Acc. Chem. Res.* **1993**, *26*, 530−536.

(8) Bunton, C. A.; Nome, F.; Quina, F. H.; Romsted, L. S. *Acc. Chem. Res.* **1991**, *24*, 357−364.

(9) Lima, J. C.; Vautier-Giongo, C.; Lopes, A.; Melo, E. C.; Quina, F. H.; Maçanita, A. L. *J. Phys. Chem. A* **2002**, *106*, 5851.

(10) Vautier-Giongo, C.; Yihwa, C.; Moreira, P. F., Jr.; Lima, J. C.; Freitas, A. A.; Quina, F. H.; Maçanita, A. L. *Langmuir* **2002**, *18*, 10109.

(11) Giestas, L.; Yihwa, C.; Lima, J. C.; Vautier-Giongo, C.; Lopes, A.; Quina, F. H.; Maçanita, A. L. *J. Phys. Chem. A* **2003**, *107*, 3263.

(12) Lima, J. C.; Abreu, I.; Santos, M. H.; Brouillard, R.; Maçanita, A. L. *Chem. Phys. Lett.* **1998**, *298*, 189.

(13) Maçanita, A. L.; Moreira, P.; Lima, J. C.; Quina, F. H.; Yihwa, C.; Vautier-Giongo, C. *J. Phys Chem. A* **2002**, *106*, 1248.

(14) Moreira, P. F., Jr.; Giestas, L.; Yihwa, C.; Vautier-Giongo, C.; Quina, F. H.; Maçanita, A. L.; Lima, J. C. *J. Phys. Chem. A* **2003**, *107*, 4203.

(15) Ferreira da Silva, P.; Lima, J. C.; Quina, F. H.; Maçanita, A. L. *J. Phys. Chem. A* **2004**, *108*, 10133.

(16) Ferreira da Silva, P.; Lima, J. C.; Freitas, A. A.; Shimizu, K.; Quina, F. H.; Maçanita, A. L. *J. Phys. Chem. A* **2005**, *109*, 7329−7338.

10.1021/la0522911 CCC: $33.50
Published on Web 12/24/2005

ground-state deprotonation of the 7-hydroxyl-4-methylflavylium cation (HMF) decreases by almost 2 orders of magnitude upon going from water (10^6 s^{-1} range) to SDS micelles (10^4 s^{-1} range), reflecting in large part the stabilization of the cationic acid form with respect to the neutral quinonoidal base.[11] The effect of micellar SDS on the excited-state proton transfer is even more pronounced, with the appearance of an additional long-lived acid form in which deprotonation is inhibited.[11]

One potential limitation of the use of simple flavylium salts such as HMF is that they are cationic and quite water-soluble and thus readily partition between the aqueous phase and the micellar phases of cationic or nonionic detergents. Partitioning of the probe can, however, be eliminated by using hydroxyflavylium salts functionalized in such a manner as to make them water insoluble.[17] In this work, we employ such a water-insoluble salt, i.e., 6-hexyl-7-hydroxy-4′-methylflavylium chloride (HHMF), to probe and compare the dynamics of proton transfer at the surface of anionic sodium dodecyl sulfate (SDS) and cationic hexadecyltrimethylammonium chloride (CTAC) micelles.

Experimental Section

Materials. The synthetic flavylium salt, 6-hexyl-7-hydroxy-4′-methylflavylium chloride (HHMF), was synthesized as previously described.[17] Sodium phosphate and bis-Tris chloride (SigmaUltra), sodium chloride (Merck p.a.), SDS (Sigma or J. T. Baker, ultrapure bioreagent grade), and CTAC (Fluka) were used without further purification.

Samples. Solutions of HHMF (ca. 10^{-5} M) were prepared in Millipore Milli-Q quality water containing 100 mM SDS or 50 or 100 mM CTAC. An appropriate buffer (typically 10 mM; sodium phosphate for SDS; bis-Tris chloride for CTAC) or HCl/NaCl (at pH <3) was employed to maintain the required pH and ionic strength in the aqueous phase of the micellar solutions. The final pH was measured by using either a Crison microp H 2002 or an Orion 720A pH meter with a combined RedRod electrode. Below pH 2, the desired hydrogen ion concentration was obtained by exact dilution of commercial perchloric acid (Riedel-de-Haen, PA 60%, or Merck, 70%) that had been previously titrated.

Absorption and Fluorescence Measurements. UV−vis absorption spectra were recorded on a Beckman DU-70, a Hewlett-Packard 8452A Diode Array, or a Shimadzu UV-2510 PC UV−vis recording spectrophotometer. Steady-state fluorescence spectra were recorded on a SPEX F212l Fluorolog or a SPEX-Jobyn Yvon Fluorolog 3 spectrofluorimeter. All fluorescence spectra are corrected.

Laser Flash Photolysis. The laser flash photolysis experiments were carried out with an Edinburgh Analytical Instruments LP900 laser flash photolysis system as previously described.[9,13] Excitation was carried out with the third harmonic (355 nm, 5 ns laser pulse width) of a Surelite II-10 Nd:YAG laser (employing a Q-Switch of 320 μs). Solutions were stirred between each laser shot, and 10 laser shots were averaged to obtain the transient absorption decays. The decays were analyzed using the Edinburgh Analytical Instruments LP900 system software. Lifetimes shorter than 30 ns were deconvoluted using the pulse shape of the laser (obtained by monitoring the Raman scattering peak of water in the fluorescence mode of the LP900). Transient absorption spectra were obtained by plotting the preexponential coefficients of the decays (or recoveries) at each wavelength.

Time-Resolved Fluorescence. Fluorescence decays were measured by the time-correlated single photon counting technique employing a Millennia Xs/Tsunami pumping system from Spectra Physics, as described elsewhere (36 ps fwhh).[11,14] The decays were deconvoluted from the excitation pulse using G. Striker's Sand program.[18]

(17) Fernandes, A. C.; et al., *Eur. J. Org. Chem.* **2004**, *23*, 4877.
(18) Striker, G.; Subramanian, V.; Seidel, C. A. M.; Volkmer, A. J. *J. Phys. Chem. B* **1999**, *103*, 8612−8617.

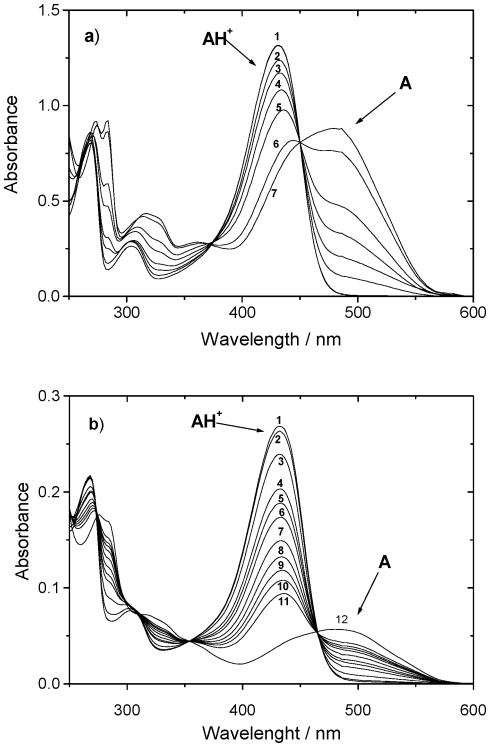

Figure 1. Absorption spectra of HHMF in (a) 100 mM SDS at pH 3.58 (1), 5.84 (2), 6.13 (3), 6.41 (4), 6.73 (5), 7.35 (6), and 7.78 (7), and (b) 100 mM CTAC at pH 0.70 (1), 1.02 (2), 1.38 (3), 1.69 (4), 1.81(5), 1.91 (6), 2.08 (7), 2.18 (8), 2.28 (9), 2.37 (10), 2.48 (11), and 3.50 (12).

Scheme 1

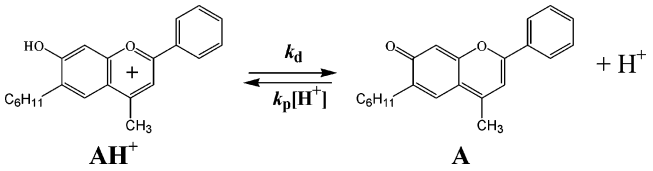

Results

Absorption Spectra. Figure 1 shows absorption spectra of aqueous solutions of HHMF in 100 mM SDS (Figure 1a) and 100 mM CTAC (Figure 1b) taken immediately (within 3 s) after preparation,[10] as a function of the pH in the intermicellar aqueous phase, pH_{aq}. The absorption spectra of HHMF in SDS (Figure 1a) exhibit the absorption band of the acid form AH^+ (see Scheme 1) at $\lambda_{max} = 431$ nm, and the absorption of the conjugate base A at $\lambda_{max} = 480$ nm. A clearly defined isosbestic point is present at 451 nm. In CTAC, the flavylium cation absorption maximum is red-shifted from 431 to 433 nm, the base maximum from 480 to 485 nm, and the isosbestic point from 451 to 465 nm.

The mole fractions of AH^+ and A, evaluated by decomposition of the spectra in Figure 1, are plotted as a function of pH_{aq} in Figure 2. The corresponding values of the apparent pK_a (referred to pH_{aq} in the intermicellar aqueous rather than to the local pH at the micelle surface) are 6.77 in 100 mM SDS (Figure 2a) and 2.03 in 100 mM CTAC (Figure 2b) at 25 °C. The apparent pK_a is much higher in micellar SDS than in CTAC, reflecting the differences in the local concentration of protons and in the stabilization of the flavylium form of the probe between anionic and cationic micelles.[10]

Transient Absorption Spectra. Figure 3a shows the transient absorption spectrum of HHMF in 100 mM SDS solution, at pH 3.85, at $t = 0$, resulting from excitation at 355 nm with a 5 ns laser pulse. The spectrum shows the depletion of AH^+ at 430

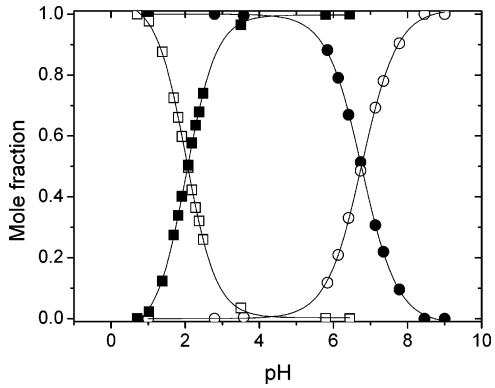

Figure 2. Mole fractions of acid (open symbols) and base (filled symbols) forms of HHMF in freshly prepared 100 mM SDS (circles) or 100 mM CTAC (squares) solutions.

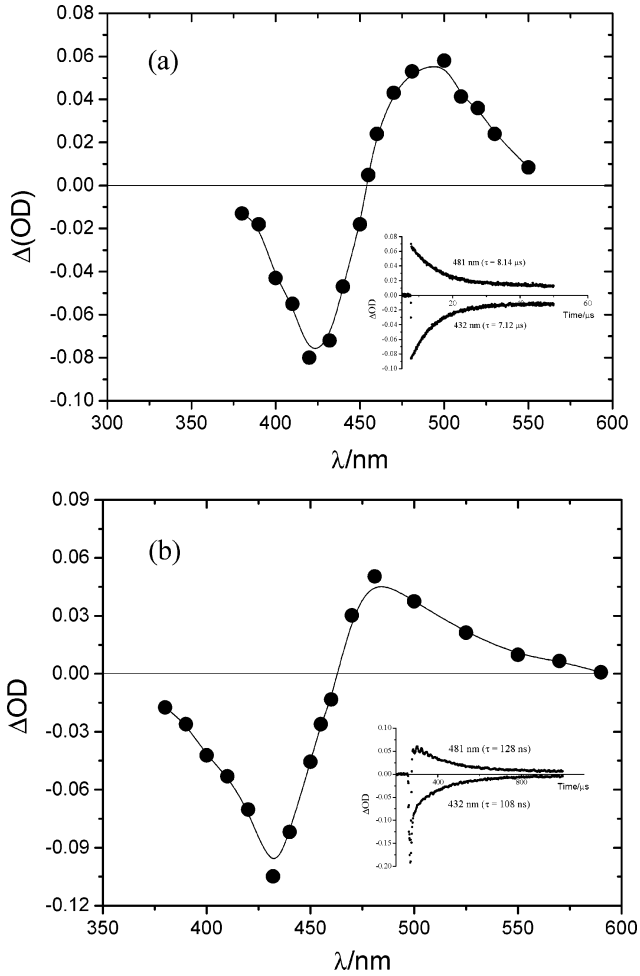

Figure 3. Transient absorption spectra of HHMF in (a) 100 mM SDS and (b) 100 mM CTAC at pH 6.40 and 1.93, respectively. The insets show transient decays and recoveries at 480 and 430 nm following excitation by a 355 nm laser pulse.

nm and an absorption band with a maximum at 480 nm that matches the absorption spectrum of A. This indicates that excitation of AH^+ leads to deprotonation of AH^+* to form the excited base A*, which then returns to the ground state A, a behavior typical of 7-hydroxyflavylium salts.[9,10,13] The decay at 480 nm and the rise time at 430 nm can be fitted with a single exponential plus a constant value (the signals do not return to zero, indicating some laser-induced photodegradation). The decay and rise times show identical values, with no significant variation with wavelength. Decreasing the pH shortens the decay (and

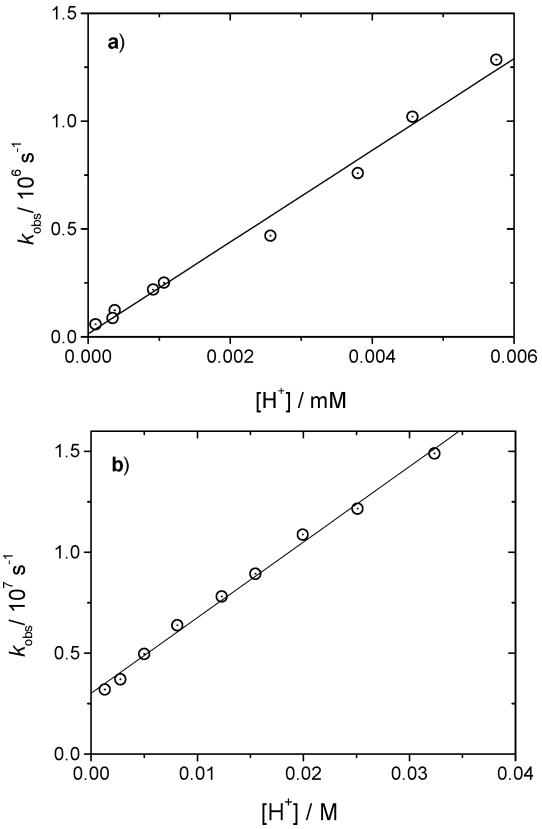

Figure 4. Plots of reciprocal equilibrium-recovery times of HHMF in (a) 100 mM SDS and (b) 100 mM CTAC.

rise) times. Similar behavior was observed for HHMF in 100 mM solutions of CTAC (Figure 3b).

Figure 4 shows plots of the observed rate constants (reciprocal decay times) in micellar SDS (Figure 4a) and CTAC (Figure 4b) as a function of the intermicellar aqueous proton concentration. The plots are linear, indicating relaxation back to the acid−base equilibrium that existed prior to the laser pulse (see Discussion section).[9,10,13]

Fluorescence Spectra. Figure 5 shows the fluorescence spectra of HHMF with excitation at the maximum of the flavylium cation absorption band (λ_{exc} = 430 and 433 nm in SDS and CTAC, respectively) in solutions of both surfactants at various pH_{aq} values. The emission of the excited acid form AH^+*, with emission maxima at 490 nm in SDS and 494 nm in CTAC, and the emission of the base form A*, with two vibronic bands at 570 and 620 nm in SDS and 580 and 640 nm in CTAC, are present over the entire range of pH_{aq}. The fluorescence spectra of HHMF are similar to those of the nonfunctionalized analogue 7-hydroxy-4-methylflavylium chloride (HMF) in micellar SDS.[11] The methoxylated compound 7-methoxy-4-methylflavylium chloride (MMF), which cannot deprotonate, shows only the cation emission band at 490 or 494 nm, respectively, in SDS or CTAC solutions.[11]

Excitation spectra of HHMF, monitored at the emission maxima of either the base or acid form, returned only the absorption spectrum of AH^+ at pH_{aq} values where the acid form is the only species present in the ground state, thus implying that A* is formed via adiabatic deprotonation of AH^+* in the excited state.

Fluorescence Decays. Fluorescence decays of HHMF in SDS or CTAC, analyzed globally at the (AH^+)* emission (490 nm) and A* emission (620 nm) maxima, are triple exponentials over the entire range of pH_{aq} investigated. Figure 6 shows representative examples of the decays and fits in SDS and CTAC. The shortest

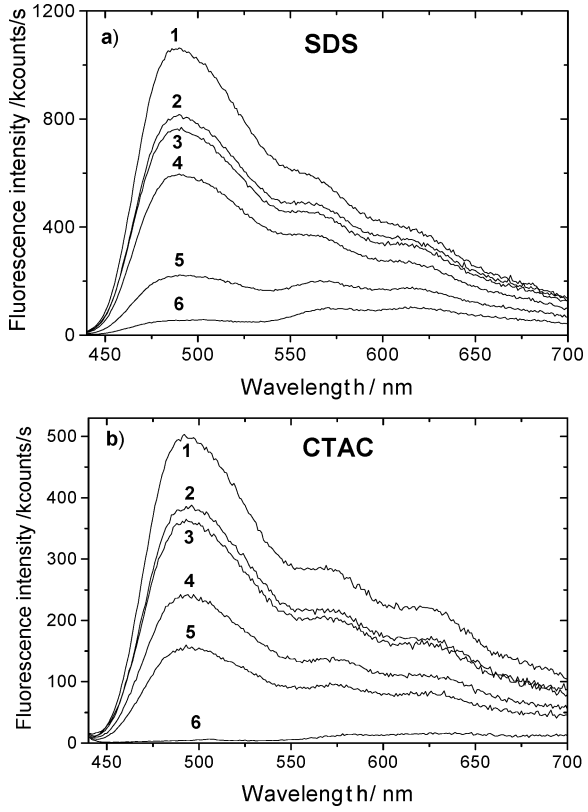

Figure 5. Fluorescence spectra of HHMF in (a) 100 mM SDS solution at pH 1.11 (1), 2.56 (2), 4.97 (3), 6.13 (4), 7.08 (5), and 7.83 (6) and (b) 50 mM CTAC solution at pH 0.18 (1), 1.49 (2), 1.88(3), 2.37 (4), 2.84 (5), and 4.88 (6). $\lambda_{exc} = 431$ nm.

lifetime τ_3 appears as a rise time at 620 nm, confirming the formation of A* in the excited state. The longest decay time τ_1 has only a small weight in the decay of A* at 620 nm and represents residual emission at 620 nm of a population of AH^{+}* that is kinetically uncoupled from A*. The pattern of the decays is similar to that found for HMF in SDS micelles, where the two shorter decay times were assigned to the kinetically coupled excited acid and base forms and the longest time was attributed to a subpopulation of the acid form incorporated into the micelle in an orientation that renders it incapable of undergoing fast deprotonation to give A*.[11]

Tables 1 and 2 summarize the decay times τ_i and preexponential coefficients A_{1i} at 490 nm for HHMF in SDS and CTAC at different pH_{aq} values. As found for HMF in SDS, the values of τ_i and A_{1i} are practically independent of pH_{aq}.[11] Particularly significant is the fact that the preexponential ratio $R = A_{13}/A_{12}$, which contains the pH_{aq} dependence of the back-protonation process ($R = \infty$ indicates that there is no back-protonation), does not exhibit appreciable variation with pH_{aq}. This means that efficient back-protonation of A*, which occurs even at pH_{aq} 7.83 in SDS, can only arise from geminate recombination of the A*−H^{+} pair resulting from deprotonation of the 7-hydroxy group of AH^{+}*. As pointed out previously,[11] the alternative possibility that water acts as the proton donor can be ruled out because A* is a weaker base than ground-state A and the latter is not protonated by water in micelles. Participation of proton-donating buffer species can be ruled out as well because they are co-ions to the micelle in all cases and the observed fluorescence decay is identical in the presence and absence of buffer at the same pH.

The behavior of HMF in SDS[11] and of HHMF in SDS and CTAC is in marked contrast to that of HMF in water, where back-protonation is diffusion-controlled and no signs of geminate

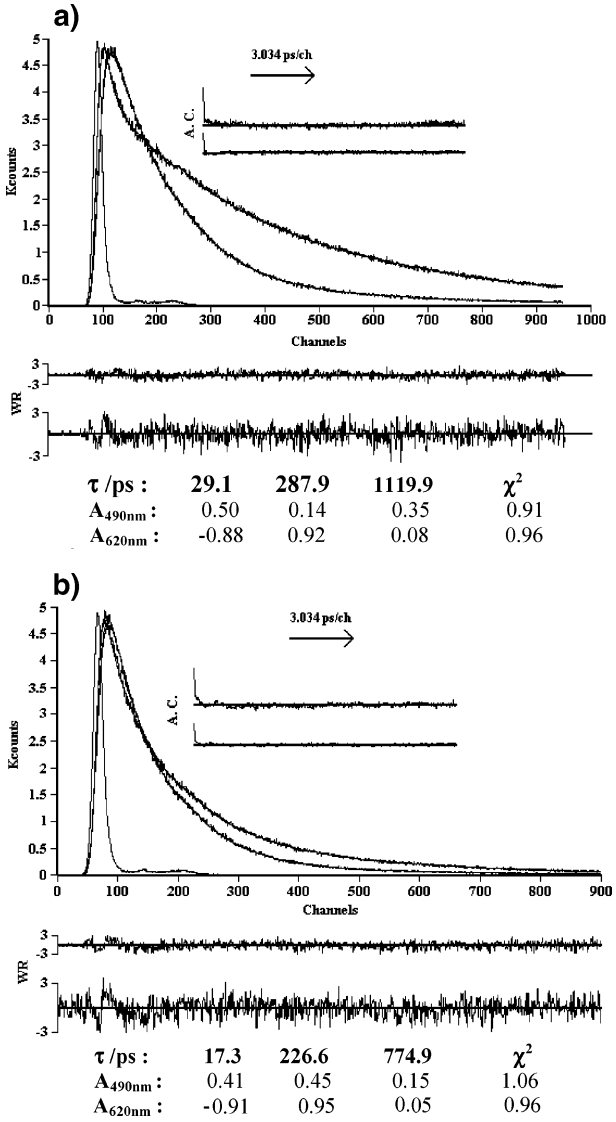

Figure 6. Fluorescence decays of HHMF in (a) 100 mM SDS solution at pH 1.5 and (b) 50 mM CTAC solution at pH 0.18.

Table 1. Decay Times τ_i and Preexponential Coefficients at 490 nm A_{1i} of HHMF in Aqueous 100 mM SDS Solutions, at 293 K, as a Function of pH

pH	τ_1/ps	τ_2/ps	τ_3/ps	A_{11}	A_{12}	A_{13}
0.52	1210	308	30	0.39	0.18	0.43
0.84	1200	300	31	0.39	0.18	0.43
0.92	1160	297	33	0.40	0.16	0.44
1.52	1110	285	30	0.37	0.15	0.48
1.92	1110	279	30	0.38	0.13	0.49
2.56	1090	279	29	0.34	0.13	0.53
3.14	1070	271	30	0.33	0.14	0.53
4.37	1100	279	31	0.34	0.13	0.53
4.97	1100	280	30	0.34	0.14	0.52
6.13	1120	277	29	0.33	0.14	0.52
7.08	1130	249	34	0.34	0.16	0.50
7.83	1130	260	38	0.32	0.15	0.53

recombination were observed. In the case of HMF, geminate recombination could only be investigated in SDS because HMF does not incorporate efficiently into cationic micelles.[11] With the water-insoluble probe HHMF, however, we find that geminate recombination occurs in both anionic and cationic micelles. The important implication is that geminate pair recombination is an intrinsic characteristic of the proton transfer process at the micelle−water interface and is insensitive to the net charge of the interface.

Table 2. Decay Times τ_i and Preexponential Coefficients at 490 nm A_{1i} of HHMF in Aqueous 50 mM CTAC Solutions, at 293 K, as a Function of pH

pH	τ_1/ps	τ_2/ps	τ_3/ps	A_{11}	A_{12}	A_{13}
0	768	225	24	0.14	0.43	0.43
0.09	767	229	32	0.15	0.44	0.41
0.18	783	225	25	0.15	0.44	0.42
0.27	787	222	22	0.15	0.46	0.39
0.36	776	228	31	0.16	0.45	0.38
0.66	789	232	26	0.16	0.43	0.42
1.03	786	221	23	0.17	0.45	0.38
1.48	782	224	25	0.16	0.40	0.45
2.12	774	230	23	0.17	0.44	0.38

In Figure 7, the effect of temperature on the decay times τ_i of HHMF in SDS at pH 2.56, and in CTAC at pH 1, is shown. All decay times decrease with increasing temperature (notably in the case of τ_1), with similar patterns in SDS and CTAC (Figure 7a,c). The major differences between the decays in the two micelles are observed in the preexponential coefficients (Figure 7b,d). Thus, the preexponential coefficient of the middle decay time, A_{12}, which accounts for the back-protonation of the base, is the smallest coefficient in SDS, but the largest in CTAC. In addition, the preexponential coefficient of the longest decay component, A_{11}, related to the fraction of the acid form of HHMF that is incapable of undergoing fast deprotonation, is much smaller in CTAC than in SDS.

Fluorescence Quenching by the Chloride Ion. The methoxylated parent compound MMF exhibits single-exponential fluorescence decay in SDS solutions[11] and in CTAC micelles above pH 2. Below ca. pH 2 in CTAC or pH 1 in SDS, the decays indicate fluorescence quenching, i.e., a shortening of the decay time, when the acidification is performed with HCl, but not when $HClO_4$ is employed. Identical quenching effects were observed when NaCl was added to CTAC solutions of MMF. Furthermore, below pH 2 in CTAC, the decays become double exponential, as a consequence of the partitioning of MMF between the aqueous and CTAC micellar phases and the different chloride ion concentrations in the two phases. At 1 M added NaCl, the decay times are reduced from 4.6 ns to 154 ps in the aqueous phase and to 51 ps in the CTAC micelle. These data are consistent with quenching by electron transfer from the chloride ion to the strongly electron accepting excited state of the cationic form of MMF.[16]

Surprisingly, the longest decay time τ_1 of HHMF in SDS or CTAC is not affected by added NaCl or HCl up to 1 M concentration, even though it is on the order of 1 ns in both micelles. Thus, the subpopulation of AH^{+}* that does not undergo fast deprotonation also does not suffer efficient electron transfer quenching by chloride ion at the micelle surface. Either this subpopulation is shielded from contact with chloride ion, or it has a lower reduction potential in the micelle. Given what is known about incorporation of solutes into micelles,[19,20] the first hypothesis is hardly plausible. Indeed, the addition of bromide ion, a much better electron donor, does result in efficient quenching of the fluorescence of HHMF in CTAC micelles. This suggests that the long-lived subpopulation of the AH^{+}* form of HHMF is embedded in a less polar micellar environment than MMF, which is sufficient to make the electron transfer from chloride ion to excited HMMF slightly endergonic.

Discussion

The shifts of the apparent pK_a's of HHMF in anionic SDS micelles (pK_{ap} = 6.77 at 100 mM SDS) and cationic CTAC micelles (pK_{ap} = 2.03 at 100 mM CTAC) are comparable to those observed for the parent compound HMF.[10] These shifts reflect both intrinsic stabilization or destabilization of AH^{+} by the charged micellar interface and the effect of the micellar electrostatic potential on the rate of protonation of A. In SDS micelles, AH^{+} is net stabilized relative to A, indicating that the electrostatic stabilization of the flavylium cation by the negative interface prevails over the "local dielectric" or micellar medium effect, which preferentially stabilizes the neutral forms relative to AH^{+}.[10] In contrast, in CTAC micelles, both electrostatic destabilization of AH^{+} and the micellar medium effect contribute to the net destabilization of AH^{+}.[10]

Ground-State Proton Transfer Kinetics. The dynamics of the ground-state proton transfer of HHMF in micellar SDS and CTAC are quite straightforward and similar to those observed for natural (anthocyanins) and synthetic flavylium salts.[9,10,13] The reciprocal of the decay (or recovery) time is equal to the sum of the deprotonation k_d and protonation $k_p[H^+]$ rate constants ($k_{obs} = k_d + k_p[H^+]$),[13] which permits determination of k_d and k_p, respectively, from the intercept and slope of plots of k_{obs} vs $[H^+]$, the concentration of protons in the intermicellar aqueous phase, as shown in Figure 4. The values of k_d are $(1.4 \pm 2.5) \times 10^4\ s^{-1}$ in 100 mM SDS and $(3.0 \pm 0.2) \times 10^6\ s^{-1}$ in 100 mM CTAC and the values of k_p are $(2.1 \pm 0.1) \times 10^{11}$ and $(3.7 \pm 0.1) \times 10^8\ M^{-1}\ s^{-1}$, respectively, in SDS and CTAC. From these values, the kinetically predicted pK_{ap}'s are 7.2 in SDS and 2.1 in CTAC. The value for SDS deviates significantly from the pK_{ap} value obtained from the mole fractions in equilibrium (6.77), due to the large error in k_d, which frequently occurs for low k_d values, i.e., when the intercept value is small compared to the $k_d + k_p[H^+]$ sum. However, a more accurate value of $k_d = 3.3 \times 10^4\ s^{-1}$ in SDS can be obtained from $k_d = k_p/K_{ap}$.

The deprotonation and protonation rate constants of HHMF in SDS and CTAC are collected in Table 3. The values of k_p reflect the differences in the charge of the surface of the two micelles: in SDS k_p increases ca. 6-fold with respect to HMF in water ($3.6 \times 10^{10}\ M^{-1}\ s^{-1}$),[10] while in CTAC it decreases 100-fold! The effect in the cationic micelle is much larger than in SDS. The values of k_d, in turn, reveal the effects of interaction with the micelle: in SDS k_d decreases 50-fold with respect to HMF in water ($1.4 \times 10^6\ s^{-1}$),[10] while in CTAC the increases is only 2-fold! Thus, while the anionic micelle surface strongly stabilizes the acid form of HHMF, CTAC only slightly destabilizes the cationic form.

Dynamics of the Long-Lived Subpopulation. The fluorescence spectra of HHMF in SDS and CTAC are similar to those of the parent compound HMF in SDS,[11] but very different from the spectrum of HMF in water, where the intensity of emission of AH^{+}* at ca. 480 nm is only residual due to fast deprotonation to water ($1.5 \times 10^{11}\ s^{-1}$).[12] In the case of HMF, the difference results from the existence in the micelle of a particular orientation of part of the population of AH^{+}* that makes these molecules unable to deprotonate to water and thus fluoresce strongly at 480 nm.[11]

The assignment of the three decay times observed in the fluorescence decay of HHMF in SDS and CTAC solutions is identical to that made for the parent compound HMF, which exhibits similar triple-exponential decays in micellar SDS:[10] τ_3 and τ_2 correspond to the kinetically coupled AH^{+}* and A* species and the longest decay time τ_1 to the subpopulation of micellar AH^{+}* that, for some reason, cannot efficiently deprotonate to water during its intrinsic lifetime. Molecules belonging to this

(19) Quina, F. H.; Alonso, E. O.; Farah, J. P. S. *J. Phys. Chem.* **1995**, *99*, 11708−11714.
(20) Sepúlveda, L.; Lissi, E.; Quina, F. *Adv. Colloid Interface Sci.* **1986**, *25*, 1−57.

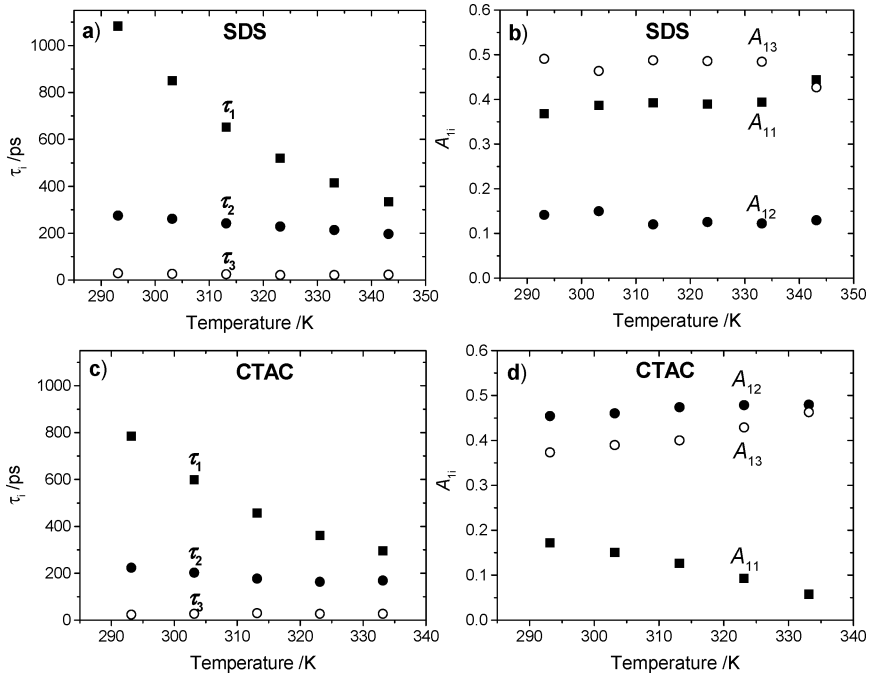

Figure 7. Plots of decay times and preexponential coefficients of HHMF in 100 mM SDS solution at pH 2.56 (a, b) and 50 mM CTAC solution at pH 1 (c, d).

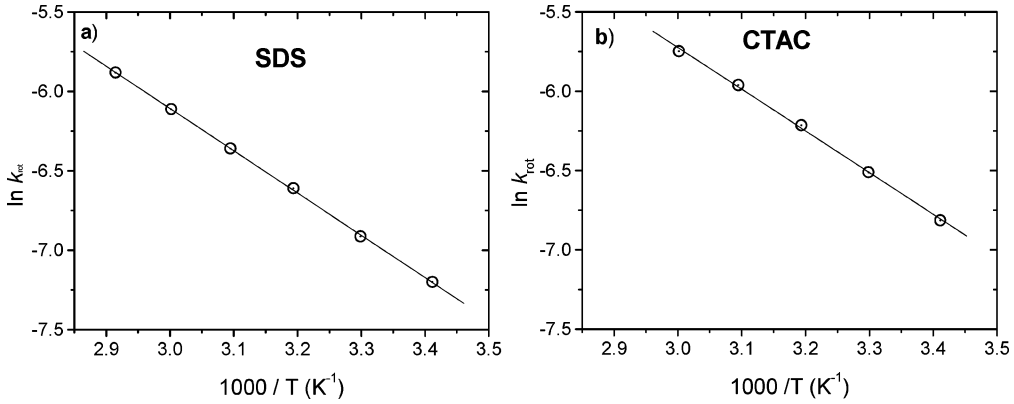

Figure 8. Arrhenius plots of rotational rate constants of HHMF in solutions of (a) 100 mM SDS at pH 2.56 and (b) 50 mM CTAC at pH 1.

Table 3. Rate Constants at 20 °C for Proton Transfer of HHMF in Micellar SDS (100 mM) and CTAC (100 mM for Ground-State Experiments, 50 mM for ESPT Experiments)

	SDS	CTAC
Ground State		
deprotonation of AH^+ (k_d/s^{-1})	3.3×10^4	3.0×10^6
protonation of A ($k_p/M^{-1}\ s^{-1}$)	2.1×10^{11}	3.7×10^8
pK_a	6.73	2.34
Excited State		
deprotonation of AH^{+}* (k_d/s^{-1})	2.5×10^{10}	2.3×10^{10}
geminate pair recombination (k_{rec}/s^{-1})	6.1×10^9	2.4×10^{10}
geminate pair dissociation (k_{diss}/s^{-1})	7.4×10^8	3.8×10^9
efficiency of pair recombination $k_r/(k_{diss}+ k_{rec})$	0.89	0.86
rotation of hindered conformer (k_{rot}/s^{-1})	7.5×10^8	1.1×10^9

last subpopulation are incorporated into the micelle in an orientation in which there is no neighboring water molecule to which the OH group of the anthocyanin can transfer the proton at the instant of excitation. These molecules must undergo molecular rotation and/or displacement in order to deprotonate, which takes several hundreds of picoseconds in the micelle at ambient temperature. Consequently, the reciprocal of τ_1 is equal to the sum of the rate constant k_{AH^+} for the decay of AH^{+}* in the absence of deprotonation and the rate constant for diffusional rotation of the acid in the micelle, k_{rot}:

$$\lambda_1 = 1/\tau_1 = k_{AH^+} + k_{rot}$$

Assuming that k_{AH^+} is equal to the reciprocal of the lifetime of the methoxylated parent compound MMF ($\tau_{MMF} = 5.6$ ns at 20 °C),[11] values of k_{rot} can be estimated from the experimental value of $1/\tau_1$. The resultant values, $7.5 \times 10^8\ s^{-1}$ in SDS and $1.1 \times 10^9\ s^{-1}$ in CTAC micelles, independent of pH, correspond to rotation times of ca. 1.3 ns in SDS and 900 ps in CTAC, in agreement with published values of rotational times in micelles at ambient temperatures.[21] The values of the apparent activation energies obtained from Arrhenius plots for k_{rot} (22.1 kJ·mol^{-1} in SDS and 21.8 kJ·mol^{-1} in CTAC micelles; Figure 8) are consistent with the range of local viscosity values typically found for ionic micelles.[5,6]

(21) (a) Chou, S. H.; Wirth, M. J. *J. Phys. Chem.* **1989**, *93*, 7694−7698. (b) Wirth, M. J.; Chou, S. H.; Piasecki, D. A. *Anal. Chem.* **1991**, *63*, 146−151. (c) Maiti, N. C.; Krishna, M. M. G.; Britto, P. J.; Periasamy, N. *J. Phys. Chem. B* **1997**, *101*, 11051−11060. (d) Carroll, M. K.; Unger, M. A.; Leach, A. M.; Morris, M. J.; Ingersoll, C. M.; Bright, F. V. *Appl. Spectrosc.* **1999**, *53*, 780−784.

Scheme 2

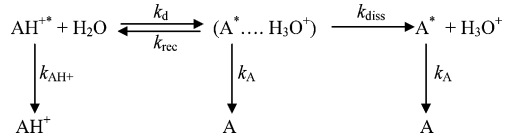

Analysis of the Coupled Acid−Base Reaction. The deprotonable fraction of micellar AH^+ gives rise to the emissions with the shorter decay times, τ_3 and τ_2. As noted in the Results section, the ratio of the preexponential coefficients A_{13}/A_{12} does not vary appreciably with pH, implying that the back-protonation of A* is pH independent. This can only arise from geminate recombination of the A^*-H^+ pair formed from deprotonation of $AH^{+}*$.[11] A schematic representation of the proposed mechanism is shown in Scheme 2,[11] whch does not include the kinetically uncoupled long-lived form of $AH^{+}*$. In this scheme, k_d represents the rate constant for deprotonation of $AH^{+}*$ to give the compartmentalized pair ($A^*\cdots H_3O^+$) at the micelle surface. This pair may, in turn, either recombine (k_{rec}) or dissociate (k_{diss}) to the free base form A*; k_{AH^+} and k_A are the reciprocal lifetimes of $AH^{+}*$ and A*.

The mechanism of Scheme 2 can be represented by the differential equation, eq 1:

$$\frac{d}{dt}\begin{bmatrix} AH^{+}* \\ A^*\cdots H^+ \\ A^* \end{bmatrix} = \begin{bmatrix} -X & k_{rec} & 0 \\ k_d & -Y & 0 \\ 0 & k_{diss} & -Z \end{bmatrix} \times \begin{bmatrix} AH^{+}* \\ A^*\cdots H^+ \\ A^* \end{bmatrix} \quad (1)$$

where X, Y, and Z are given by eqs 2−4.

$$X = k_d + k_{AH^+} \quad (2)$$

$$Y = k_{rec} + k_{diss} + k_A \quad (3)$$

$$Z = k_A \quad (4)$$

Equation 1 predicts triple-exponential decay functions for the three species ($AH^{+}*$, compartmentalized pair, and A*), where the three reciprocal decay times (λ_i), corresponding to the roots of eq 5, are given by eqs 6 and 7.

$$\begin{vmatrix} \lambda - X & k_{rec} & 0 \\ k_d & \lambda - Y & 0 \\ 0 & k_{diss} & \lambda - Z \end{vmatrix} = 0 \quad (5)$$

$$\lambda_{3,2} = \frac{X + Y \pm \sqrt{(X-Y)^2 + 4k_{rec}k_d}}{2} \quad (6)$$

$$\lambda_A = k_A \quad (7)$$

As found for the parent compound HMF, two of the three decay times predicted by Scheme 2 (τ_2 and k_A) are not experimentally distinguishable.[11] The rate constants were calculated from the decay times ($\tau_i = 1/\lambda_i$) and the preexponential ratios ($R = A_{13}/A_{12}$) via eqs 8−12, and their values are presented in Table 3.

$$X = \frac{R\lambda_3 + \lambda_2}{R+1} \quad (8)$$

$$Y = \lambda_3 + \lambda_2 - X \quad (9)$$

$$k_d = X - k_{AH^+} \approx X \quad (10)$$

$$k_{rec} = \frac{XY - \lambda_3\lambda_2}{k_d} \quad (11)$$

$$k_{diss} = Y - k_A - k_{rec} \quad (12)$$

The rate constants in Table 3 were used to simulate the values of the reciprocal decay times and the preexponential coefficients from pH 1 to 7. The results confirm that λ_2 and $1/k_A$ are experimentally undistinguishable over this pH range (either the two times are too close to each other or one of the preexponential coefficients is too small). This means that the compartmentalized pair is revealed in this system only through the abnormal pH dependence of the protonation reaction and not by the presence of an additional exponential term in the fluorescence decays.

There are two important pieces of information in Table 3 concerning the effect of micellization on deprotonation and geminate recombination. In the ground state, the value of k_d in CTAC is 2 orders of magnitude larger than in SDS, reflecting respectively the destabilizing and stabilizing effects of the micellar surface on the ground-state reaction-controlled deprotonation. In contrast, in the excited state the values of the rate constants k_d for deprotonation of $AH^{+}*$ are practically identical in SDS ($2.5 \times 10^{10}\ s^{-1}$) and CTAC ($2.3 \times 10^{10}\ s^{-1}$). Thus, the stabilization (SDS) and or destabilization (CTAC) of the cation in the ground state does not influence the excited-state deprotonation. In both micelles, the value of k_d for the excited state decreases about the same relative to water ($1.5 \times 10^{11}\ s^{-1}$ for HMF).[12] The obvious implication is that the excited-state deprotonation is not reaction controlled. In the case of HMF and some other flavylium salts in water, deprotonation of $AH^{+}*$ is in fact controlled by the dielectric (Debye) relaxation time of water.[14] Consequently, the decrease of k_d at the micelle surface must result from either a decreased availability of protonable water or a lower water mobility at the micelle surface.[4]

The second interesting piece of information is provided by the values of the recombination k_{rec} and dissociation k_{diss} rate constants of the compartmentalized geminate pair. The two rate constants are, respectively, 4- and 5-fold larger in CTAC than in SDS, indicating substantially greater proton mobility in the cationic micelle. Nonetheless, recombination occurs with high net efficiency in both micelles (0.86 in CTAC and 0.89 in SDS).

Conclusions

The functionalized flavylium cation HHMF has been employed to probe some of the fundamental aspects of proton transfer reactions in micelles, without interference from water−micelle partitioning of the probe. The fact that the alkyl chain of HHMF anchors it to the cationic CTAC micelle allowed a clean comparison between the dynamics of proton transfer at the surfaces of CTAC and SDS micelles. Because the proton transfer reactions of anthocyanins can be accompanied in both the ground and excited states, micellar effects on prototropic reactions can be probed on the time scale from picoseconds to microseconds with HHMF. Although not specifically treated in this work, HHMF has shown interesting potential as a probe of fast electron transfer reactions in micelles and other compartmentalized media.

Micellar stabilization or destabilization of HHMF does not affect the fast proton transfer reactions in the excited state (picosecond time range), but the deprotonation rates are significantly reduced in the micelle with respect to water (ca. 6-fold), due to decreased availability or mobility of water at the micelle surface. Interestingly, the rate constants are quite similar

in SDS and CTAC. Micellar stabilization/destabilization of the flavylium cation does, however, affect the slower ground-state proton transfer reactions (typically in the nanosecond to microsecond time range), reducing the deprotonation rate in anionic SDS micelles and increasing it in cationic CTAC micelles. At the micelle surface geminate ($A^*\cdots H^+$) pairs have a finite existence and geminate pair recombination is efficient even for ($A^*\cdots H^+$) pairs in which the base is neutral. Moreover, the effect is similar in both anionic and cationic micelles. Simplistically, one might have expected that the negatively charged micellar surface would retard the proton escape and thus enhance recombination, while the positively charged micellar surface would be expected to do the contrary. Although the reasoning may be basically correct ($k_{diss}(SDS) < k_{diss}(CTAC)$), the micelle charge also affects the recombination rate about equally ($k_{rec}(SDS) < k_{rec}(CTAC)$), the net result being that the overall efficiency of recombination remains the same in cationic and anionic micelles.

Acknowledgment. This work was supported by the FCT, Portugal (Project No. POCTI/QUI/38884/2001), CNPq, Brazil, and ICCTI/CAPES/423. F.H.Q. thanks the CNPq for fellowship and grant (Universal 475337/2004-2) support.

LA0522911